

Multifractal Measures of $M \geq 3$ Shallow Earthquakes in the Taipei Metropolitan Area

Jeen-Hwa Wang^{1,*}, Kou-Cheng Chen¹, Win-Gee Huang¹, Kao-Hao Chang¹, Jeng-Cheng Wang²,
and Pei-Ling Leu³

¹*Institute of Earth Sciences, Academia Sinica, Taipei, Taiwan*

²*Department of Applied Geoinformatics, Chia-Nan University of Pharmacy and Science, Tainan City, Taiwan*

³*Seismological Center, Central Weather Bureau, Taipei, Taiwan*

Received 18 March 2013, accepted 9 September 2013

ABSTRACT

The generalized fractal dimensions are measured for $M \geq 3$ shallow earthquakes with focal depths of ≤ 40 km in the Taipei Metropolitan Area (from 121.3 to 121.9°E and 24.8 to 25.3°N) over the 1973 - 2010 period based on spatial distribution (using epicentral and hypocentral distances between two events, r) and time sequence (using the inter-event time between two events, t). The multifractal measures are estimated from log-log plots of $C_q(r)$ versus r and $C_q(t)$ versus t , where $C_q(r)$ and $C_q(t)$ are the generalized correlation integral, respectively, of r and t at positive q . For the spatial distribution, $C_q(r)$ is calculated based on the epicentral distance (i.e., the 2D measure) and hypocentral distance (i.e., the 3D measure). Under both 2D and 3D measures, the log-log plot of $C_q(r)$ versus r shows a linear distribution when $\log(r_o) \leq \log(r) \leq \log(r_{ub})$ and roll-over when $r > r_{ub}$. For all cases $\log(r_o)$ is 0.3, and $\log(r_{ub})$ are 1.7 and 1.4 for the 2D and 3D measures, respectively. D_q , which is the slope of the linear portion, monotonically decreases with increasing q , thus indicating that the epicentral and hypocentral distributions of earthquakes are multifractal. The values of D_q are lower than 2 and 3, respectively, for the 2D and 3D measures. For the time sequence of the events in study, $C_q(t)$ is calculated based on the inter-event time between two events. The log-log plot of $C_q(t)$ versus t does not seem able to show a linear relationship in a large range of $\log(r)$ or r and the value of D_q cannot be evaluated, thus suggesting that the time sequence of $M \geq 3$ shallow earthquakes in the Taipei Metropolitan Area (TMA) is not multifractal.

Key words: Earthquakes, Epicentral and hypocentral distributions, Inter-event time, Multifractal

Citation: Wang, J. H., K. C. Chen, W. G. Huang, K. H. Chang, J. C. Wang, and P. L. Leu, 2014: Multifractal measures of $M \geq 3$ shallow earthquakes in the Taipei metropolitan area. *Terr. Atmos. Ocean. Sci.*, 25, 17-26, doi: 10.3319/TAO.2013.09.09.01(T)

1. INTRODUCTION

In 1944, the frequency-magnitude relation reported by Gutenberg and Richter (1944) was the first scaling law to represent self-similarity of earthquake phenomena. Other studies also led to a conclusion that self-similarity or scale-invariance is a common property of natural phenomena. Mandelbrot (1983) proposed the concepts of fractal geometry and fractal dimension to describe the scale-invariant natural phenomena. This concept has been widely applied to describe the spatial distribution of earthquakes (cf. Turcotte 1989; Hirabayashi et al. 1992; Wang and Lin 1993; Wang and Lee 1996; Wang and Shen 1999) and time series

of earthquakes (Smalley et al. 1987; Hirata 1989; Kagan and Jackson 1991; Ogata and Abe 1991; Papadopoulos and Dedousis 1992; Koyama et al. 1995; Wang and Lee 1995; Wang 1996) and fault activities (cf. Aviles et al. 1987; Okubo and Aki 1987; Lee and Schwarcz 1995).

A fractal set is defined to be one for which the Hausdorff-Besicovitch dimension strictly exceeds the commonly used topological dimension (Mandelbrot 1983). The fractal dimension is a characteristic index of a fractal set. However, it is not easy to apply the Hausdorff-Besicovitch definition to estimate the fractal dimension in the real world. Several alternatives to estimate the fractal dimension have been suggested (cf. Takayasu 1990). A similarity dimension D_S is defined for an exactly self-similar set as $D_S = \log(L)/\log(N)$,

* Corresponding author
E-mail: jhwang@earth.sinica.edu.tw

where L is the linear size and N is the number of the similar daughters. Capacity dimension D_{CA} is defined as $D_{CA} = \log[N(r)]/\log(1/r)$, where $N(r)$ is the smallest number of covering of a set with a size of r . The information dimension D_I is defined to be $D_I = \sum p_i(r) \log[p_i(r)]/\log(r)$, where r is the distance between two points, on the basis of the probabilistic distribution $p_i(r)$, which will be described below. The correlation dimension D_C is defined from the correlation integral $C(r)$ in the following relation: $C(r) \sim r^{D_C-d}$, where d is the spatial (or topological) dimension (2 and 3 for the 2D and 3D spaces) and $C(r)$ is defined for the epicentral distribution $\{r_i\}$ ($i=1, 2, 3, \dots, N$) as

$$C(r) = 2N(R < r)/N(N - 1) \quad (1)$$

where $N(R < r)$ is the number of pairs of events with a distance $R < r$ (cf. Grassberger and Procaccia 1983). In general, $D_S = D_{CA} \geq D_I \geq D_C$, and D_C is the smallest value of the four fractal dimensions. The equality $D_S = D_{CA} = D_I = D_C$ holds only in the case of a homogeneous fractal set. Most natural fractals are not completely self-similar and are actually multifractal. For such fractals, $D_S = D_{CA} > D_I > D_C$. Hence, a single value of fractal dimension is not sufficient to characterize the multifractal properties. Therefore, the idea of fractal dimension has been extended to a generalized fractal or multi-fractal dimension, D_q (Grassberger 1983; Hentshe and Procaccia 1983). Wang and Lee (1995) proposed that a $D_q - q$ relation rather than the first three values of D_q can completely represent multifractal behavior of a time series.

Taiwan is situated in the collision boundary between the Philippine Sea and Eurasian plates (Tsai et al. 1977; Wu 1978; Lin 2002). The former moves northwestward with a speed of about 8 cm year⁻¹ (Yu et al. 1997). The Philippine Sea plate is subducting underneath the Eurasian plate in northern Taiwan, where the Taipei Metropolitan Area (TMA) is located. The active collision and subduction has resulted in high seismicity in the Taiwan region (Wang et al. 1983; Wang 1998; Wang and Shin 1998). From 1972 to 1991, the Taiwan Telemetered Seismographic Network (TTSN), sponsored by the National Science Council (NSC), was operated by the Institute of Earth Sciences (IES), Academia Sinica to monitor earthquakes in Taiwan. This network consists of 24 stations, each equipped with a vertical high-gain velocity seismometer. The earthquake magnitude used by the TTSN was the duration magnitude. Wang (1989a) described this network in detail. Since 1991, the old seismic network of Central Weather Bureau (CWB) has been upgraded and many new stations have been added to form a new network, i.e., the CWB Seismic Network (CWBSN). In 1992 the TTSN was merged into the CWBSN. The earthquake magnitude of the earthquake catalogue has been unified to be the local magnitude. A detailed description about the CWBSN can be found in Shin (1992) and Shin and Chang (2005); only a brief de-

scription is given below. At present, the CWBSN consists of 72 stations, each equipped with a three-component velocity seismometer. The seismograms are recorded in both high- and low-gain forms. This network provides high-quality digital earthquake data to the seismological community. The uncertainty of earthquake location is 2 km for the epicenter and 5 km for the focal depth.

The TMA is the political, economic, and cultural center of Taiwan. Hence, seismic risk mitigation in the area has drawn much attention. For this purpose, seismicity of the area should be investigated in depth. A description about the geology of the TMA can be found in several articles (e.g., Wang and Lin 1993; Chang et al. 1998; Teng et al. 2001; Wang et al. 2006) and will not be given here. The seismicity and related seismic problems in the TMA were studied based on data obtained by the TTSN, CWBSN, and several portable seismic arrays by several researchers (e.g., Tsai et al. 1977; Wu 1978; Wang et al. 1983, 1994, 2006, 2011, 2012a, 2012b; Wang 1988; Chen and Yeh 1991; Wang and Shen 1999; Lin 2002, 2005; Kim et al. 2005; Konstantinou et al. 2007). A brief review can be found in Wang et al. (2006) and Wang (2008).

Wang et al. (2006) investigated the epicentral distribution, depth distribution, and temporal sequences of $M \geq 4$ earthquakes occurred from 1973 - 2005. They divided the earthquakes into two groups, with a depth difference of about 20 km: one for shallow events with focal depths ranging 0 - 40 km and the other with focal depths larger than 60 km. The deep events occurred along the subduction zone with a dip angle of about 70°. Shallow earthquakes were located primarily in a depth range from 0 - 10 km north of 25.1°N, and down to 35 km in depth for those south of 25.1°N. After 1988, no $M \geq 4$ shallow event was located within this area. Deep events occurred more or less uniformly during the study time period. The annual number of shallow earthquakes decreased with time from 1973 to 1988, and varies year from year for deep events. In addition, the frictional rupture/quasi-plastic (FR/QP) transition model is applied to interpret the depth distribution of shallow earthquakes. Wang et al. (2012a) applied three statistical models, the gamma, power-law, and exponential functions, to describe the single frequency distribution of inter-event times between two consecutive events for both shallow and deep earthquakes with $M \geq 3$ in the TMA from 1973 to 2010. Results show that among the three functions, the power-law function is the most appropriate one for describing the data points. The scaling exponent of the power-law function decreases linearly with an increasing lower-bound magnitude. The slope value of the regression equation is smaller for shallow earthquakes than for deep events. Meanwhile, the power-law function does not work when the threshold magnitude is 4.2 for shallow earthquakes and 4.3 for deep event. Wang et al. (2012b) studied the memory effect, which represents the long- or short-term correlation between two events in an area, in the $M \geq 3$ earthquakes which

occurred in the TMA from 1973 through 2010 by applying the fluctuation analysis technique. For both shallow and deep earthquakes, three magnitude ranges, i.e., $M \geq 3$, $M \geq 3.5$, and $M \geq 4$, are considered. Calculated results show that the exponents of the scaling law of fluctuation versus window length for all earthquakes sequences in consideration are not larger than 0.5, thus suggesting that the $M \geq 3$ earthquakes in the TMA are short-term correlated.

Wang and Lin (1993) and Wang and Lee (1996) measured the generalized fractal dimensions at positive q based on the epicentral distances for the $M \geq 1$ earthquakes in west Taiwan. They observed that earthquakes in the region exhibit fractal properties. All D_q 's are smaller than 2 and D_q is higher in southwest Taiwan than in northwest Taiwan. In other words, seismicity is more homogeneous in the former than in the latter. Wang and Lee (1995) and Wang (1996) proposed a method to measure the generalized fractal dimensions of time series of earthquakes. Wang (1996) measured the generalized fractal dimensions at positive q for $M \geq 7$ earthquakes in Taiwan. He observed that only the values of D_q can be measured only for $q < 7$, even though the time series of those earthquakes is multifractal.

In this study, we will measure the generalized fractal dimensions (as defined below) of $M \geq 3$ shallow earthquakes with focal depths ≤ 40 km occurred in the TMA from 1973 to 2010 in the space and time domains. In the spatial domain, both the epicentral and hypocentral distances are taken into account.

2. DATA

From shallow earthquakes occurring in the TMA from 1973 to 1984, Wang (1988) obtained $b = 1.33 \pm 0.13$ in the magnitude range of 1.8 - 3.3. For the eastern part of TMA, Wang (1989b) observed $b = 1.21 \pm 0.01$ for the events in the magnitude range of 2.1 - 4.8 which occurred from 1973 to 1985. From shallow earthquakes occurring in the Tatun Volcano Group (TVG) from 1973 to 1999, Kim et al. (2005) estimated $b = 1.22 \pm 0.05$ for the magnitude range 2.1 - 3.5. Their results show that the earthquake data should be complete when the data reach $M > 2$ in the study area. However, only $M \geq 3$ earthquakes which occurred in the area (from 121.3 to 121.9°E and 24.8 to 25.3°N) from 1973 to 2010 are taken into account for the following reasons: (1) the ability of detecting earthquakes with $M < 3$ is lower for deep events than shallow ones; and, (2) $M \geq 3$ earthquakes must be more significant than $M < 3$ events for the problem of seismic risk mitigation, because damage caused by $M < 3$ events are usually very small. The earthquake data are retrieved directly from the CWB's data base. The number of events used in this study is 874. The maximum location uncertainty is ~ 2 km horizontally and ~ 5 km vertically. The location uncertainty essentially increases with depth and is higher for offshore earthquakes than for inland events.

Since the deep earthquakes occurred at the geometrically concaved subduction zone (see Wang et al. 2006), they are not appropriate for the evaluation of D_q in this study. Hence, only the shallow events are considered below. Wang et al. (2006) observed that shallow earthquakes have focal depths mainly in the range of 0 - 10 km north of 25.1°N and down to 40 km south of 25.1°N. Wang (1989b) and Wang et al. (2006) also found that in the eastern part of the TMA, the earthquakes can be located down to a depth of 40 km. The shallow events to the north of 25.1°N are located mainly at the TVG. Wang et al. (1994, 2006) observed that except for the earthquakes in the subduction zone, the events occurring in northern Taiwan are usually shallow. Kim et al. (2005) also obtained similar results. The epicenters of shallow earthquakes used in this study are plotted in Fig. 1. This figure shows a heterogeneous distribution of epicenters. There are three areas with higher seismicity. The first one is inland and around the TVG. The second one is offshore to the northeast of the TMA. The third one is offshore to the southeast of the TMA.

Figure 2 shows a time sequence of earthquake magnitudes. The shortest inter-event time between adjacent events is less than 1 day; while the longest inter-event time is 925.4 days. Since a few events occurred in a short time interval apart, e.g., a day, the line segments representing them are not clearly separable. Hence, those events are displayed by a line segment with the largest earthquake magnitude. It is obvious that the temporal variation in earthquakes before 1988 is different from that after 1988. The frequency of events was higher before 1988 than after 1988. Clearly, after 1988 only an $M > 4$ shallow event was located in the TMA.

3. GENERALIZED FRACTAL DIMENSION

Generalized fractal dimension D_q is defined by the following expression:

$$D_q = \lim [\log(\sum p_i^q) / \log(\delta)] / (q - 1) \quad (2)$$

where p_i is the probability that an event falls into a box with a length l (Grassberger 1983; Hentschel and Procaccia 1983). The parameter q can take any real number in the range from $-\infty$ to ∞ . D_q of large, positive q shows the fractal property of dense regions, where p_i is large, and D_q of large, negative q displays that of thin regions, where p_i is small. D_q for negative q can take a value larger than the spatial dimension d (2 and 3 for the 2D and 3D spaces, respectively), thus calling D_q a dimension makes no geometric sense for $D_q > d$ (Mandelbrot 1989). For an object, the value of D_q at small q shows the fractal property of a coarse structure and that at large q exhibits the fractal property of a fine structure. For $q \geq 0$, the largest D_q is D_0 and D_q decreases with increasing q . When the $D_q - q$ relations of two objects are the

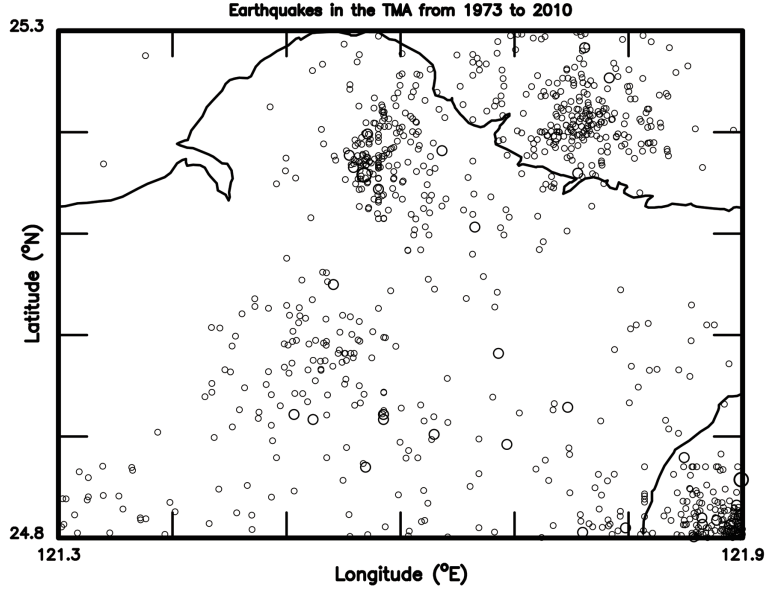


Fig. 1. Epicenters (in open circles) of $M \geq 3$ shallow earthquakes with focal depths ≤ 40 km. Different sizes of circles show the magnitudes of earthquakes.

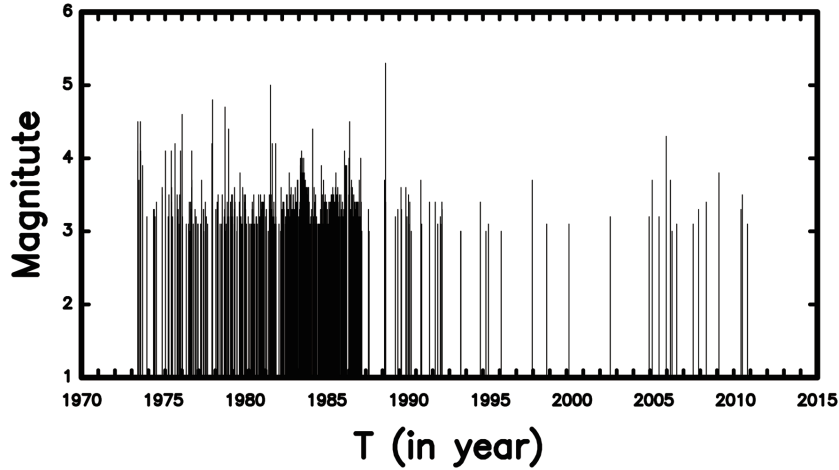


Fig. 2. Time sequences of magnitudes of $M \geq 3$ shallow earthquakes with focal depths ≤ 40 km.

same, they are considered statistically similar. For $q = 0, 1,$ and $2, D_q$ relates to the capacity dimension D_{CA} , information dimension D_I , and correlation dimension D_C , respectively. The probability p_i can be estimated by the box-counting method from the observed data. However, the box-counting method requires a large number of data. An alternative correlation integral method was suggested by Kurths and Herzog (1987). A local density function $n_j(r)$ is defined by the following expression:

$$n_j(r) = \sum_k \Theta(r - |\mathbf{r}_j - \mathbf{r}_k|) / (N - 1) \quad (3)$$

where the value of $\Theta(s)$ is 1 if $s \geq 0$ and 0 if $s < 0$. In Eq. (3), \mathbf{r}_j and \mathbf{r}_k are the position vectors of events j and k , re-

spectively, and thus $|\mathbf{r}_j - \mathbf{r}_k|$ is the distance between the two points $(\mathbf{r}_j, \mathbf{r}_k)$. The vector \mathbf{r}_i is denoted by $\langle x_i, y_i, z_i \rangle$, where $x_i, y_i,$ and $z_i,$ represent the latitude multiplied by 111 km, longitude multiplied by 111 km, and focal depth (in km), respectively. The value of 111 km is the length of 1° for both latitude and longitude on the ground surface (Öncel et al. 1996). Hence, a generalized correlation integral $C_q(r)$ for the distance between two events, r , is defined by

$$C_q(r) = [\sum n_j^{q-1}(r)]^{1/(q-1)} \quad (4)$$

$C_q(r)$ is considered to be related to r in the following form:

$$C_q(r) \sim r^{D_q} \quad (5)$$

In this study, two methods for measuring the distance are used. The first one is

$$r_{jk} = |\mathbf{r}_j - \mathbf{r}_k| = [(x_j - x_k)^2 + (y_j - y_k)^2]^{1/2} \quad (6)$$

and, thus is called the 2D measure. The second one is

$$r_{jk} = |\mathbf{r}_j - \mathbf{r}_k| = [(x_j - x_k)^2 + (y_j - y_k)^2 + (z_j - z_k)^2]^{1/2} \quad (7)$$

and, thus is called the 3D measure.

It should be noted that Hirata (1989) used the following formula to calculate r_{jk} : $r_{jk} = \cos\phi^{-1}[\cos\theta_j\cos\theta_k + \sin\theta_j\sin\theta_k\cos(\phi_j - \phi_k)]$, where θ_i and ϕ_i are, respectively, the co-latitude and longitude of event i , on the spherical surface. Some researchers (e.g., Öncel et al. 1996; Telesca et al. 2001; Marquez-Ramirez et al. 2012) also used this formula to calculate the distance between two events. Since the study areas used by Hirata (1989) (7 degrees along the south-north direction and 5 degrees along the east-west direction), Öncel et al. (1996) (7 degrees along the south-north direction and > 11 degrees along the east-west direction), Telesca et al. (2001) (2 degrees along both the south-north and east-west directions), and Marquez-Ramirez et al. (2012) (4 degrees along the north-south direction and 5 degrees along the east-west direction for the Colima, Mexico earthquakes and 5 degrees along the north-south direction and 7 degrees along the east-west direction for the Landers earthquake sequence, USA) were large, a spherical triangle should be taken into account. The three groups of researchers also converted the degree of angle to the distance using $1^\circ = 111$ km (Öncel et al. 1996). However, since the area of this study is quite small ($< 0.5^\circ$ along the two directions), it does not seem necessary to consider a spherical triangle. Hence, our calculations based on Eq. (7) should be acceptable.

In order to study multifractal behavior of time series of earthquakes, Wang and Lee (1995) replaced the two spatial quantities by a time interval t and an inter-event time $|t_i - t_k|$, respectively. Hence, a generalized correlation integral $C_q(t)$ for the inter-event time, t , is

$$C_q(t) = [\sum n_j^{q-1}(t)]^{1/(q-1)} \quad (8)$$

$C_q(t)$ is considered to be related to t in the following form:

$$C_q(t) \sim t^{D_q} \quad (9)$$

The log-log plots of $C_q(r)$ versus r and $C_q(t)$ versus t at different q 's will be first constructed. Then the value of D_q will be calculated from the linear portion of data points. In this study, only the values of D_q at positive q 's are calcu-

lated because we are only interested in the fractal properties of denser areas.

Telesca et al. (2001) and Marquez-Ramirez et al. (2012) stressed that it is necessary to examine stability of evaluated values of multi-fractal dimensions. Telesca et al. (2001) applied the Allan factor to examine the significance of temporal variation in fractal dimension in different time windows. However, since we do not study the temporal variation in multi-fractal dimensions in this study, we do take their results into account. On the other hand, for the spatial distribution of events Marquez-Ramirez et al. (2012) studied in detail the effects of numbers of data on stability and significance of estimated multi-fractal dimensions from both simulation events under different models and natural earthquakes. Their results are quite significant and can meet the basic concept of fractal geometry. From simulation results, they addressed the need to obtain stable evaluations of D_q ; the number of samples should be large. Such numbers are also dependant on the model in consideration. The larger the number in use, the more stable is the evaluated value. Stable evaluations can lead to significant multi-fractal dimensions. Meanwhile, the evaluated values for fractal objects are obviously different from those from non-fractal objects. In general, the numbers are ≥ 1000 for D_0 and D_1 and ≥ 800 for D_2 . In addition, based upon earthquakes which occurred in Colima, Mexico and Landers, USA they found that the evaluated values of D_0 , D_1 and D_2 are stable and significant when the numbers of events are larger than 1600, 1000, and 300, respectively, for D_0 , D_1 and D_2 for the earthquakes in Colima and 500 for D_0 , D_1 and D_2 for the events in Landers. Although they examine the significance of evaluated values only for D_0 , D_1 and D_2 , they also concluded that the number of samples must be, at least, higher than 600 for evaluations of D_q 's when $q > 2$. Hence, their results are directly applied to this study. The number of events used by this study is 874. In addition, D_2 is equal to the correlation dimension, D_C , which directly represents the fractal property of an object of a set of objects. Hence, for stable evaluations of multi-fractal dimensions D_q is measured only for $q \geq 2$ for the study area.

4. RESULTS

For the multifractal measures in the space domain, the maximum distances are 78.42 km (for the epicentral distance) and 108.61 km (for the hypocentral distance) under the 2D and 3D measures, respectively. The generalized correlation integral functions, C_q , versus the distance, r , between two earthquakes at $q = 2, \dots$ and 15 are calculated from the data set. Since the data points are close to one another for large q 's, the log-log plots of $C_q(r)$ versus r are displayed only at $q = 2, 5, 8, 11$, and 14. Results are displayed in Fig. 3 under the 2D measure and in Fig. 4 under the 3D measure. Since the uncertainty of the epicenter is 2 km as mentioned

above, the smallest distance, r_0 , is taken to be 2 km, thus giving $\log(r_0) = 0.3$. Actually, the uncertainty of the focal depth is about 5 km. However, for the 3D measures there is only one data point with $r < 5$ km. The only one data point cannot make a significant effect on the estimate of scaling exponent. Hence, the minimum distance r is still taken to be 2 km for the 3D cases. The largest distance, r_c , is set to be 82 km, which is between 78.42 and 108.61 km, thus $\log(r_c) = 1.92$. Li et al. (1994) suggested that the upper bound of the linear portion, r_1 , is taken to be 30 or 50% of the largest distance to avoid the possible existence of roll-over. According to their criterion, the value of r_c of this study must be shorter than 82 km. Nevertheless, here r_c is still taken to be 82 km to display the

possible existence of roll-over. Hence, the data points are plotted in the range of $0.3 \leq \log(r) \leq 1.92$. The degree of scattering of data points is higher in Fig. 4 than in Fig. 3. It can be seen from Figs. 3 and 4 that when $0.3 \leq \log(r) \leq 1.7$, the data points are well distributed around a linear trend; while when $\log(r) > 1.7$, the pattern of data points is roll-over. The value of r_1 is $10^{1.7} = 50.1$ km, which is 60% of $r_c = 82$ km, 64% of 78.42 km (under the 2D measures), and 46% of 108.61 km (under the 3D measures). Since the percentages are comparable with those by Li et al. (1994), the evaluated results could be acceptable.

The least-squared method is applied to infer a linear regression equation to fit the linear portion of data points. D_q is just the slope value of the linear equation. The values of D_q at $q = 2, \dots, 15$ and their standard deviations are listed in Table 1. Since the deviations of D_q for all q 's and all cases in this study are not higher than 0.005, the evaluated values of D_q are considered reliable. The obtained $D_q - q$ relations are shown in Fig. 5: solid circles for the 2D measures and open circles for the 3D measures. D_q essentially decreases with increasing q . The differences in the values of D_q between the 2D and 3D measures are only slightly independent on q .

For the measures in the time domain, the maximum inter-event time is 37.28 yrs. The generalized correlation integral functions, C_q , versus inter-event time, t , in years between two earthquakes at $q = 2, \dots$ and 15 are calculated for the data set. For the space domain, the log-log plots of $C_q(r)$ versus r at $q = 2, 5, 8, 11$, and 14 are displayed in Fig. 6. The data points are plotted in the range $0.3 \leq \log(t) \leq 1.6$.

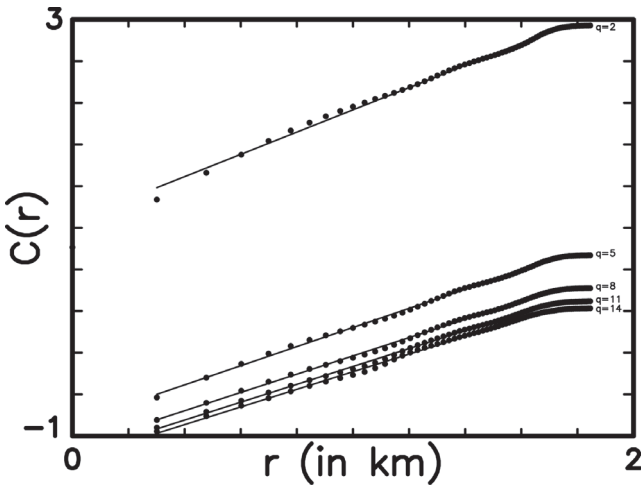


Fig. 3. The log-log plots of $C_q(r)$ versus r at $q = 2, 5, 8, 11$, and 14 for $M \geq 3$ shallow earthquakes in the study area under the 2D measures. The solid lines represent the regression lines inferred from the data points with $0.3 \leq \log(r) \leq 1.7$.

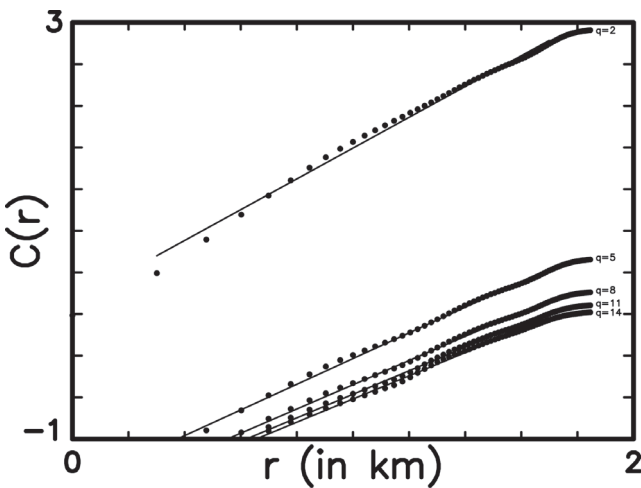


Fig. 4. The log-log plots of $C_q(r)$ versus r at $q = 2, 5, 8, 11$, and 14 for $M \geq 3$ shallow earthquakes in the study area under the 3D measures. The solid lines represent the regression lines inferred from the data points with $0.3 \leq \log(r) \leq 1.7$.

Table 1. The values of D_q with standard errors at $q = 2, \dots, 15$ for the study area under the 2D and 3D measures.

q	2D measures	3D measures
02	1.069 ± 0.002	1.478 ± 0.003
03	0.987 ± 0.001	1.349 ± 0.002
04	0.944 ± 0.001	1.278 ± 0.002
05	0.918 ± 0.001	1.234 ± 0.002
06	0.900 ± 0.001	1.203 ± 0.002
07	0.887 ± 0.001	1.181 ± 0.001
08	0.878 ± 0.001	1.164 ± 0.001
09	0.870 ± 0.001	1.150 ± 0.001
10	0.863 ± 0.001	1.139 ± 0.001
11	0.858 ± 0.001	1.131 ± 0.001
12	0.854 ± 0.001	1.123 ± 0.001
13	0.850 ± 0.001	1.117 ± 0.001
14	0.847 ± 0.001	1.113 ± 0.001
15	0.844 ± 0.001	1.108 ± 0.001

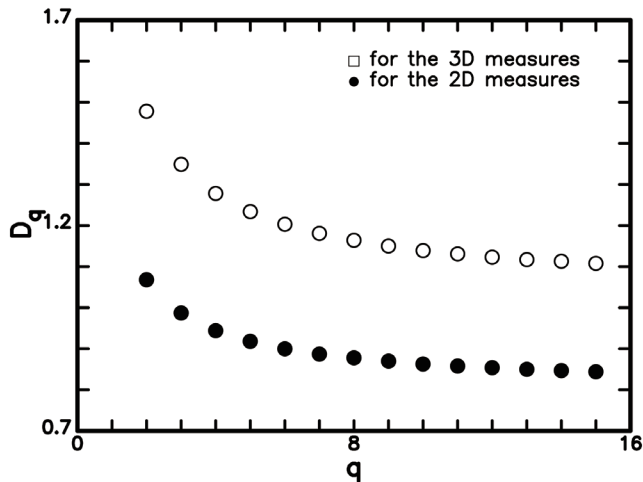


Fig. 5. The plot of D_q versus q : solid circles for the 2D measure and open circles for the 3D measure.

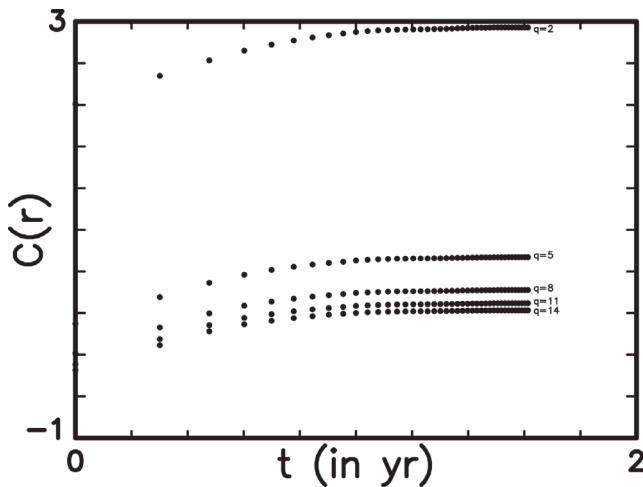


Fig. 6. The log-log plots of $C_q(t)$ versus t at $q = 2, 5, 8, 11,$ and 14 for $M \geq 3$ shallow earthquakes in the study area.

The upper bound for inter-event time is $10^{1.6} = 41$ yrs. Obviously, the data points are well distributed around a linear trend only in a small range of small $\log(r)$. Hence, the value of D_q cannot be evaluated from the figure.

5. DISCUSSION

From Figs. 3 to 6 for the spatial distributions of earthquakes, it can be seen that the log-log plots of $C_q(r)$ versus r show a linear pattern when $0.3 \leq \log(r) \leq 1.7$ under both the 2D and 3D measures. Results clearly suggest that the epicentral and hypocentral distributions of $M \geq 3$ earthquakes in the TMA are multifractal. Nevertheless, the linear pattern of data points does not appear in the whole range of r or $\log(r)$. This means that the size of the study area actually influences multifractal behavior. This can also be seen

from the results posted by Wang and Lee (1996). The upper bound of r (denoted by r_{ub}) of the linear portion is ~ 50 km ($= 10^{1.7}$ km). The length along the longitude and that along the latitude are 88 and 55 km, respectively. Obviously, $r_{ub} = 50$ km is almost the length of the whole area along the latitude. Figure 1 shows that the epicenters are distributed almost throughout the entire ranges along the longitude and latitude. Hence, the value of r_{ub} is comparable to the length of the study area. As mentioned above, the pattern of data points is roll-over when $\log(r) > 1.7$. This phenomenon indicates that the value of $\log(C_q)$ for $\log(r) > 1.7$ is less than that estimated from the linear regression equation deduced from the data points with $0.3 \leq \log(r) \leq 1.7$. This is actually caused by the finite size of the study area.

Telesca et al. (2001) and Marquez-Ramirez et al. (2012) stressed that it is necessary to examine significance of evaluations of multi-fractal dimensions. Marquez-Ramirez et al. (2012) provided significant results obtained from natural earthquakes and simulation events under different models. Their results are directly applied to examine significance of evaluations of D_q 's of this study. To resolve the problem, it is necessary to compare results from evaluations with those from the null hypothesis. The hypothesis proposed by Marquez-Ramirez et al. (2012) is taken into account. Their hypothesis is that the seismogenic processes generated by the stress field under the geologic characteristics result in seismicity with a fractal, spatially distribution. On the other hand, their null hypothesis is that the fractal dimensions are evaluated from non-fractal distributions of points, e.g., from a random spatial distribution with uniform probability. Their results as displayed in Fig. 3 show that the grid and uniform distributions are apparently monofractal, while the observed seismicity distributions are clearly multifractal. In fact, the dimension of a non-fractal distribution increases as the number of points (its density) increases, while that of a fractal distribution remains constant. Hence, their results suggest that the null hypothesis can be rejected. Our evaluations are similar to theirs. According to their studies, the evaluated fractal dimensions of this study are significant.

The spatial (or topological) dimensions of the 2D and 3D spaces are 2 and 3, respectively. From Table 1, we can see that for the two areas in consideration, the values of D_q evaluated under the 2D measures are lower than 1.3 and much smaller than 2; and those under the 3D measure are lower than 1.7 and much smaller than 3. This means that there are many voids in the space of study as shown in Fig. 1, and thus the generalized fractal dimensions are much smaller than the related spatial (or topological) dimensions.

Wang and Lin (1993) and Wang and Lee (1996) measured the generalized fractal dimensions at positive q based on the epicentral distances for the $M \geq 1$ earthquakes in west Taiwan (including the north and south zones and three sub-zones in the former and two subzones in the latter). They observed that earthquakes in the region exhibit a fractal

property. All D_q 's are smaller than 2 and D_q higher in south zone than in north zone. The value of r_{ub} is 25 km for the north zone and 40 km for the south zone and 12 km for three subzones in the north zone. They found that the values of $r_{ub} = 25$ and 40 km are almost the smallest widths of epicentral distributions of the north and south zones, respectively, and the value of $r_{ub} = 12$ km is almost the smallest size of cluster of epicenters of subzones of the north zone. The values of D_q range from 1.0 to 1.3 for the north zone and from 1.4 to 1.6 for the south zone. Considering the 2D measures for the study area as listed in Table 1 and displayed in Fig. 5, the values of D_q of this study are smaller than those measured by Wang and Lee (1996) for earthquakes in the north and south zones in west Taiwan. The present values are also smaller than those of the subzones of the two zones. It is noted that the smallest magnitude was 1 for the earthquakes used by Wang and Lee (1996) and is 3 for the events of this study. We assume that when smaller events in the TMA are taken into account, the values of D_q should increase.

Figure 6 reveals that for the time sequence in study, the log-log plots of $C_q(t)$ versus t do not exhibit a linear portion in a large range of $\log(t)$ and thus the $D_q - q$ relation is not evaluated. This suggests that the time sequence of $M \geq 3$ earthquakes in the TMA does not show a fractal property. The reason is still open. For the seismicity of the New Hebrides between mid-1978 and mid-1984, Smalley et al. (1987) observed that the fractal dimension varies from 0.126 to 0.255 and the earthquake occurrences significantly deviate from random or Poisson behavior. Kagan and Jackson (1991) stated that for 1-D processes, if the correlation dimension equals to 1 over all time periods from zero to infinity, the process is Poissonian. For global seismicity, they also found that long-term, weak clustering characterizes all mainshock earthquakes and is governed by a power-law temporal distribution. They also mentioned that the fractal dimension of the set of earthquakes on the time axis is of the order of 0.8 - 0.9, thus, the mainshock occurrence is closer to a stationary Poisson process. The fractal dimension used by these authors is the correlation dimension and equivalent to D_2 in this study. The value of D_2 cannot be evaluated from the present time series of earthquakes. Hence, in comparison with previous studies, the component of the Poisson processes is weak in the present time sequence of earthquakes. As mentioned above, Wang et al. (2012a) found that among the three functions, i.e., exponential-law, power-law and gamma functions, the power-law function is the most appropriate one for describing the time sequence of $M \geq 3$ earthquakes in the TMA. Obviously, the present conclusion of multifractal measures is consistent with theirs. Wang (1996) measured the values of D_q for 44 $M \geq 7$ earthquakes during the 1900 - 1994 period in the Taiwan region (latitude of 20 to 26°N and longitude of 119 to 124°E) based on a complete catalogue compiled by Wang and Kuo (1995). Wang (1996) found that the log-log plots of $C_q(t)$ versus t are poor-

ly distributed when $q \geq 7$, and thus only the value of D_q for $q < 7$ could be measured. Nevertheless, $M \geq 7$ earthquakes in Taiwan still show multifractal behavior, at least, for the coarse structures of time sequence. Obviously, the time sequence of $M \geq 3$ shallow earthquakes in the TMA is quite different from that of $M \geq 7$ earthquakes in Taiwan.

6. CONCLUSION

The generalized fractal dimensions are measured for the $M \geq 3$ shallow earthquakes with focal depths ≤ 40 km in the TMA (from 121.3 to 121.9°E and 24.8 to 25.3°N) during the 1973 - 2010 period based on the spatial distribution (using the epicentral and hypocentral distances between two events, r) and time series (using the inter-event time between two events, t). In the space domain, the maximum epicentral and hypocentral distances are 78.42 and 108.61 km, respectively, for the whole area and 75.66 and 98.59 km, respectively, for the smaller area. Multifractal measures are made from the log-log plots of $C_q(r)$ versus r and $C_q(t)$ versus t . To examine the size of a study area on multifractal measures, the earthquakes in a smaller area are also taken into account. For the spatial distribution, $C_q(r)$ is calculated from the epicentral and hypocentral distances. Under both 2D and 3D measures of C_q , the log-log plots of $C_q(r)$ versus r show a linear distribution of data points when $\log(r_0) \leq \log(r) \leq \log(r_{ub})$ and roll-over when $\log(r) > \log(r_{ub})$. For all cases $\log(r_0)$ is 0.3, and $\log(r_{ub})$ is 1.7 for the 2D measures and 1.4 for the 3D measures. D_q , which is the slope of the linear portion, is a well-distributed, monotonically decreasing function of q , thus indicating that the epicentral and hypocentral distributions of earthquakes show multifractal behavior. The values of D_q are much smaller than 2 and 3 for the 2D and 3D measures, respectively. D_q is higher under the 3D measures than under the 2D measures. In the time domain, the maximum inter-event time is 37.28 yrs. The log-log plot of $C_q(t)$ versus t does not show a linear distribution in a large range of $\log(t)$, and thus the value of D_q cannot be evaluated. This suggests that the time sequence of $M \geq 3$ shallow earthquakes in the TMA is not multifractal.

Acknowledgements The authors would like to thank Prof. C.-C. Chen (Associate Editor of TAO), Prof. J.-M. Chiu (Memphis State University, USA) and an anonymous reviewer for their useful comments to substantially improve the article. They also thank the Central Weather Bureau for providing earthquake data. This work was sponsored by Academia Sinica (Taipei) and the National Science Council under Grant No. NSC100-2119-M-001-015.

REFERENCES

Aviles, C. A., C. H. Scholz, and J. Boatwright, 1987: Fractal analysis applied to characteristic segments of the

- San Andreas fault. *J. Geophys. Res.*, **92**, 331-344, doi: 10.1029/JB092iB01p00331. [[Link](#)]
- Chang, H. C., C. W. Lin, M. M. Chen, and S. T. Lu, 1998: An introduction to the active faults of Taiwan, Explanatory Text of the Active Fault Map of Taiwan SCALE 1:55000, Central Geol. Surv., MOEA, ROC, 103 pp. (in Chinese)
- Chen, K. J. and Y. H. Yeh, 1991: Gravity and microearthquake studies in the Chinshan-Tanshui area, northern Taiwan. *Terr. Atmos. Ocean. Sci.*, **2**, 35-50.
- Grassberger, P., 1983: Generalized dimensions of strange attractors. *Phys. Lett.*, **97A**, 227-230, doi: 10.1016/0375-9601(83)90753-3. [[Link](#)]
- Grassberger, P. and I. Procaccia, 1983: Measuring the strangeness of strange attractors. *Phys. Nonlinear Phenom.*, **9**, 189-208, doi: 10.1016/0167-2789(83)90298-1. [[Link](#)]
- Gutenberg, B. and C. F. Richter, 1944: Frequency of earthquakes in California. *Bull. Seismol. Soc. Am.*, **34**, 185-188.
- Hentschel, H. G. E. and I. Procaccia, 1983: The infinite number of generalized dimensions of fractals and strange attractors. *Phys. Nonlinear Phenom.*, **8D**, 435-444, doi: 10.1016/0167-2789(83)90235-X. [[Link](#)]
- Hirabayashi, T., K. Ito, and T. Yoshii, 1992: Multifractal analysis of earthquakes. *Pure Appl. Geophys.*, **138**, 591-610, doi: 10.1007/BF00876340. [[Link](#)]
- Hirata, T., 1989: A correlation between the *b* value and the fractal dimension of earthquakes. *J. Geophys. Res.*, **94**, 7507-7514, doi: 10.1029/JB094iB06p07507. [[Link](#)]
- Kagan, Y. Y. and D. D. Jackson, 1991: Long-term earthquake clustering. *Geophys. J. Int.*, **104**, 117-133, doi: 10.1111/j.1365-246X.1991.tb02498.x. [[Link](#)]
- Kim, K. H., C. H. Chang, K. F. Ma, J. M. Chiu, and K. C. Chen, 2005: Modern seismic observations in the Tatun volcano region of northern Taiwan: Seismic/volcanic hazard adjacent to the Taipei Metropolitan area. *Terr. Atmos. Ocean. Sci.*, **16**, 579-594.
- Konstantinou, K. I., C. H. Lin, and W. T. Liang, 2007: Seismicity characteristics of a potentially active Quaternary volcano: The Tatun Volcano Group, northern Taiwan. *J. Volcanol. Geotherm. Res.*, **160**, 300-318, doi: 10.1016/j.jvolgeores.2006.09.009. [[Link](#)]
- Koyama, J., S. X. Zang, and T. Ouchi, 1995: Mathematical modeling and stochastic scaling of complex earthquake activity. In: Koyama, J. and D. Feng (Eds.), *Advance in Mathematical Seismology*, Seismological Press, Beijing, 165-180.
- Kurths, J. and H. Herzel, 1987: An attractor in a solar time series. *Phys. Nonlinear Phenom.*, **25D**, 165-172, doi: 10.1016/0167-2789(87)90099-6. [[Link](#)]
- Lee, H. K. and H. P. Schwarcz, 1995: Fractal clustering of fault activity in California. *Geology*, **23**, 377-380, doi: 10.1130/0091-7613(1995)023<0377:FCOFAI>2.3.CO;2. [[Link](#)]
- Li, D., Z. Zheng, and B. Wang, 1994: Research into the multifractal of earthquake spatial distribution. *Tectonophysics*, **233**, 91-97, doi: 10.1016/0040-1951(94)90222-4. [[Link](#)]
- Lin, C. H., 2002: Active continental subduction and crustal exhumation: The Taiwan orogeny. *Terr. Nova*, **14**, 281-287, doi: 10.1046/j.1365-3121.2002.00421.x. [[Link](#)]
- Lin, C. H., 2005: Seismicity increase after the construction of the world's tallest building: An active blind fault beneath the Taipei 101. *Geophys. Res. Lett.*, **32**, L22313, doi: 10.1029/2005GL024223. [[Link](#)]
- Mandelbrot, B. B., 1983: *The Fractal Geometry of Nature*, W. H. Freeman and Company, New York, 468 pp.
- Mandelbrot, B. B., 1989: Multifractal measures, especially for the geophysicist. *Pure Appl. Geophys.*, **131**, 5-42, doi: 10.1007/BF00874478. [[Link](#)]
- Márquez-Rámirez, V. H., F. A. N. Pichardo, and G. Reyes-Dávila, 2012: Multifractality in seismicity spatial distributions: Significance and possible precursory applications as found for two cases in different tectonic environments. *Pure Appl. Geophys.*, **169**, 2091-2105, doi: 10.1007/s00024-012-0473-9. [[Link](#)]
- Ogata, Y. and K. Abe, 1991: Some statistical features of the long-term variation of the global and regional seismic activity. *Int. Stat. Rev.*, **59**, 139-161.
- Okubo, P. G. and K. Aki, 1987: Fractal geometry in the San Andreas fault system. *J. Geophys. Res.*, **92**, 345-355, doi: 10.1029/JB092iB01p00345. [[Link](#)]
- Öncel, A. O., I. Main, Ö. Alptekin, and P. Cowie, 1996: Spatial variations of the fractal properties of seismicity in the Anatolian fault zones. *Tectonophysics*, **257**, 189-202, doi: 10.1016/0040-1951(95)00132-8. [[Link](#)]
- Papadopoulos, G. A. and V. Dedousis, 1992: Fractal approach of the temporal earthquake distribution in the Hellenic arc-trench system. *Pure Appl. Geophys.*, **139**, 269-276, doi: 10.1007/BF00876331. [[Link](#)]
- Shin, T. C., 1992: Some implications of Taiwan tectonic features from the data collected by the Central Weather Bureau Seismic Network. *Meteorol. Bull. CWB*, **38**, 23-48. (in Chinese)
- Shin, T. C. and J. S. Chang, 2005: Earthquake monitoring systems in Taiwan. In: Wang, J. H., C. Y. Wang, Q. C. Song, T. C. Shin, S. B. Yu, C. F. Shieh, K. L. Wen, S. L. Chung, M. Lee, K. M. Kuo, and K. C. Chang (Eds.), *The 921 Chi-Chi Major Earthquake*, Office of Inter-Ministry S&T Program for Earthquake and Active-fault Research, NSC, 43-59. (in Chinese)
- Smalley, R. F. Jr., J. L. Chatelain, D. L. Turcotte, and R. Prévot, 1987: A fractal approach to the clustering of earthquakes: Applications to the seismicity of the New Hebrides. *Bull. Seismol. Soc. Am.*, **77**, 1368-1381.
- Takayasu, H., 1990: *Fractals in the Physical Sciences*, Manchester University Press, Manchester, 170 pp.
- Telesca, L., V. Cuomo, V. Lapenna, and M. Macchiato,

- 2001: Identifying space-time clustering properties of the 1983-1997 Irpinia-Basilicata (Southern Italy) seismicity. *Tectonophysics*, **330**, 93-102, doi: 10.1016/S0040-1951(00)00221-3. [[Link](#)]
- Teng, L. S., C. T. Lee, C. H. Peng, W. F. Chen, and C. J. Chu, 2001: Origin and geological evolution of the Taipei Basin Northern Taiwan. *Western Pacific Earth Sci.*, **1**, 115-142.
- Tsai, Y. B., T. L. Teng, J. M. Chiu, and H. L. Liu, 1977: Tectonic implications of the seismicity in the Taiwan region. *Mem. Geol. Soc. China*, **2**, 13-41.
- Turcotte, D. L., 1989: Fractals in geology and geophysics. *Pure Appl. Geophys.*, **131**, 171-196, doi: 10.1007/BF00874486. [[Link](#)]
- Wang, C. Y. and T. C. Shin, 1998: Illustrating 100 years of Taiwan seismicity. *Terr. Atmos. Ocean. Sci.*, **9**, 589-614.
- Wang, J. H., 1988: *b* values of shallow earthquakes in Taiwan. *Bull. Seismol. Soc. Am.*, **78**, 1243-1254.
- Wang, J. H., 1989a: The Taiwan Telemetered Seismographic Network. *Phys. Earth Planet. Inter.*, **58**, 9-18, doi: 10.1016/0031-9201(89)90090-3. [[Link](#)]
- Wang, J. H., 1989b: Aspects of seismicity in the southernmost part of the Okinawa trough. *Proc. Geol. Soc. China*, **32**, 79-99.
- Wang, J. H., 1996: Multifractal measures of time series of $M \geq 7$ earthquakes in Taiwan. *J. Geol. Soc. China*, **39**, 117-123.
- Wang, J. H., 1998: Studies of earthquake seismology in Taiwan during the 1897-1996 period. *J. Geol. Soc. China*, **41**, 291-336.
- Wang, J. H., 2008: Urban seismology in the Taipei Metropolitan Area: Review and Prospective. *Terr. Atmos. Ocean. Sci.*, **19**, 213-233, doi: 10.3319/TAO.2008.19.3.213(T). [[Link](#)]
- Wang, J. H. and H. C. Kuo, 1995: A catalogue of $M_s \geq 7$ Taiwan earthquakes (1900-1994). *J. Geol. Soc. China*, **38**, 95-106.
- Wang, J. H. and W. H. Lin, 1993: A fractal analysis of earthquakes in west Taiwan. *Terr. Atmos. Ocean. Sci.*, **4**, 457-462.
- Wang, J. H. and C. W. Lee, 1995: Multifractal characterization of an earthquake sequence. *Phys. Stat. Mech. Appl.*, **221**, 152-158.
- Wang, J. H. and C. W. Lee, 1996: Multifractal measures of earthquakes in west Taiwan. *Pure Appl. Geophys.*, **146**, 131-145, doi: 10.1007/BF00876673. [[Link](#)]
- Wang, J. H. and H. Y. Shen, 1999: Multifractal measures of epicentral distribution of $M \geq 6$ earthquakes in the north-south seismic belt of Mainland China. *J. Geol. Soc. China*, **42**, 631-637.
- Wang, J. H., Y. B. Tsai, and K. C. Chen, 1983: Some aspects of seismicity in Taiwan region. *Bull. Inst. Earth Sci., Acad. Sin.*, **3**, 87-104.
- Wang, J. H., K. C. Chen, and T. Q. Lee, 1994: Depth distribution of shallow earthquakes in Taiwan. *J. Geol. Soc. China*, **37**, 125-142.
- Wang, J. H., M. W. Huang, and W. G. Huang, 2006: Aspects of $M \geq 4$ earthquakes in the Taipei metropolitan area. *Western Pacific Earth Sci.*, **6**, 169-190.
- Wang, J. H., K. C. Chen, S. J. Lee, and W. G. Huang, 2011: The 15 April 1909 Taipei earthquake. *Terr. Atmos. Ocean. Sci.*, **22**, 91-96, doi: 10.3319/TAO.2010.08.16.01(T). [[Link](#)]
- Wang, J. H., K. C. Chen, S. J. Lee, W. G. Huang, Y. H. Wu, and P. L. Leu, 2012a: The frequency distribution of inter-event times of $M \geq 3$ earthquakes in the Taipei Metropolitan Area: 1973 - 2010. *Terr. Atmos. Ocean. Sci.*, **23**, 269-281, doi: 10.3319/TAO.2011.12.20.01(T). [[Link](#)]
- Wang, J. H., K. C. Chen, S. J. Lee, W. G. Huang, and P. L. Leu, 2012b: Fluctuation analyses of $M \geq 3$ earthquake sequences in the Taipei Metropolitan Area. *Terr. Atmos. Ocean. Sci.*, **23**, 633-645, doi: 10.3319/TAO.2012.08.14.01(T). [[Link](#)]
- Wu, F. T., 1978: Recent tectonics of Taiwan. *J. Phys. Earth*, **2**, S265-S299.
- Yu, S. B., H. Y. Chen, and L. C. Kuo, 1997: Velocity field of GPS stations in the Taiwan area. *Tectonophysics*, **274**, 41-59, doi: 10.1016/S0040-1951(96)00297-1. [[Link](#)]